

Preparing non-local superpositions of quasi-classical light states

A. Ourjoumtsev, F. Ferreyrol, R. Tualle-Broui and P. Grangier

*Laboratoire Charles Fabry de l'Institut d'Optique,
CNRS, Univ. Paris Sud,*

RD128, 91127 Palaiseau, France

(Dated: September 11, 2008)

Schrödinger cat states of the light [1], defined as quantum superpositions of quasi-classical (coherent) states, have recently emerged as an interesting alternative to single-photon qubits for quantum information processing (QIP) [2–6]. Their richer structure provides significant advantages for quantum teleportation, universal quantum computation, high-precision measurements or fundamental physics tests [7–13]. Local superpositions of free-propagating coherent states have been realized experimentally, but their applications were so far limited by their extreme sensitivity to losses, and by the lack of quantum gates for coherent qubit rotations. We demonstrate a simple approach to generate strongly entangled *non-local* superpositions of coherent states, using a very lossy quantum channel. They can be used to implement a coherent qubit rotation gate, and to teleport those qubits over long distances. This scheme can be extended to create entangled coherent superpositions with arbitrarily large amplitudes.

Single-mode cat states can be considered as classical light waves with two opposite phases simultaneously, expressed as $\mathcal{C}(|\alpha\rangle + e^{i\phi} |-\alpha\rangle)$, where $|\alpha\rangle$ is a coherent state containing $|\alpha|^2$ photons on average, and \mathcal{C} is a normalization factor omitted in the following. Their non-classical nature appears most strikingly on the quantum statistics of the electric field: its quasi-probability distribution, called Wigner function, presents quantum oscillations with negative values between the two classical states. The Wigner function $W(x, p)$, where $\hat{x} = \frac{1}{\sqrt{2}}(\hat{a} + \hat{a}^\dagger)$ and $\hat{p} = \frac{1}{i\sqrt{2}}(\hat{a} - \hat{a}^\dagger)$ are the quadrature operators of the quantized electric field, can be reconstructed by homodyne tomography [14] from several marginal distributions $P_\theta(x_\theta = x \cos \theta + p \sin \theta)$.

Besides their fundamental interest, arbitrary coherent superpositions $a|\alpha\rangle + b|-\alpha\rangle$ can be used as qubits carrying quantum information, if $|\alpha\rangle$ and $|-\alpha\rangle$ are sufficiently distinguishable ($|\alpha|^2 \gtrsim 2$). They present many advantages compared to discrete-variable qubits $a|0\rangle + b|1\rangle$, allowing one to circumvent the fundamental limits of discrete-variable quantum teleportation [7, 15] or to perform loophole-free Bell tests [13].

So far, their applications suffered from two major issues. One was the difficulty to build associated logic gates: arbitrary qubit rotations were believed to re-

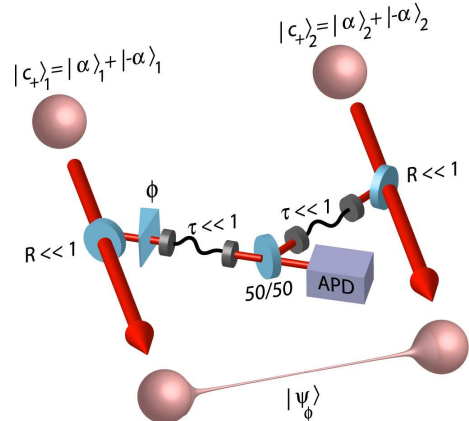


FIG. 1: Entanglement of two independent cat states $|c_+\rangle_{1,2}$ using non-local photon subtraction through lossy channels. When small fractions R of each pulse, phase-shifted by ϕ , interfere on a 50/50 beamsplitter, an APD photon detection in one of the outputs prepares the entangled state $|\psi_\phi\rangle$ (Eq. 1), useful as a resource for long-distance quantum teleportation and phase-space rotations of coherent qubits (see text for details).

quire either unrealistically strong non-linear interactions, or very resource-consuming repeated infinitesimal rotations [8, 13]. The other was more fundamental: the complex structure of these states, while offering many benefits, makes them notoriously fragile. For instance, many QIP tasks require entangled cat states such as $|\psi_0\rangle = |\alpha\rangle_1 |-\alpha\rangle_2 - |-\alpha\rangle_1 |\alpha\rangle_2$. Theoretically, they can be obtained by splitting a single-mode cat $|\sqrt{2}\alpha\rangle - |-\sqrt{2}\alpha\rangle$ on a 50/50 beamsplitter (BS) and sending the two output modes to distant sites. But even small losses ϵ decrease the fidelity with the pure state as $-\epsilon|\alpha|^2$: transmitting cats with a large “size” $|\alpha|^2$ becomes increasingly difficult. When $\epsilon > 1/2$ (~ 15 km of optical fiber) the negativity of the Wigner function, and hence the quantum character of the state, disappears.

The approach demonstrated here circumvents the fragility of these states, typically described with continuous quadrature variables, by using the robustness offered by discrete-variable QIP. It consists in probabilistic entanglement swapping, similar to the discrete-variable DLCZ protocol [16], where losses decrease the success rate instead of the state quality. We create long-range entanglement by subtracting a delocalized single photon from initially separable states, which can be manipulated

locally and remain protected from losses. We show that the success rate and the quality of the prepared states are independent on their size $|\alpha|^2$. In addition to long-distance quantum teleportation, they can be used to rotate a coherent qubit by an arbitrary angle with a simple photon counting measurement.

The protocol is illustrated on Fig. 1. Two single-mode cat states $|c_{\pm}\rangle_{1,2} = |\alpha\rangle_{1,2} + |-\alpha\rangle_{1,2}$ are prepared locally on two distant sites 1 and 2. A small fraction of each is reflected and sent through the lossy quantum link on a 50/50 beamsplitter (BS). One of the subtracted beams is dephased by ϕ before interfering, and one of the BS outputs is monitored with a single photon detector (avalanche photodiode, APD). A detection event heralds the subtraction of a single photon delocalized between the two modes 1 and 2 [17], applying the annihilation operator $\hat{a}_1 - e^{i\phi}\hat{a}_2$. Since $\hat{a}(|\alpha\rangle \pm |-\alpha\rangle) = |\alpha\rangle \mp |-\alpha\rangle$, we prepare the strongly entangled coherent superposition

$$|\psi_{\phi}\rangle = -i \sin \frac{\phi}{2} |\alpha\rangle_1 |\alpha\rangle_2 - \cos \frac{\phi}{2} |-\alpha\rangle_1 |\alpha\rangle_2 \\ + \cos \frac{\phi}{2} |\alpha\rangle_1 |-\alpha\rangle_2 + i \sin \frac{\phi}{2} |-\alpha\rangle_1 |-\alpha\rangle_2 \quad (1)$$

The generated state is essentially unaffected by the losses in the quantum channel, as long as the success rate exceeds the APD dark counts (as shown below, this is true even for long distances). For $\phi = 0$, this is the ‘‘coherent Bell state’’ $|\psi_0\rangle$ above, proposed as a resource to teleport coherent qubits $|\xi\rangle = a|\alpha\rangle + b|-\alpha\rangle$ [7, 18]: mixing $|\xi\rangle$ with the mode 1 on a 50/50 BS and counting photons in the output ports projects the mode 2 into $|\xi\rangle$, with the usual bit- and phase-flips depending on which combination of numbers (0,even), (0,odd), (even,0) or (odd,0) was measured. The only other possible outcome (0,0), corresponding to a failure, occurs with a probability $\sim e^{-2|\alpha|^2}$ and rapidly becomes negligible.

The crucial advantage of the states $|\psi_{\phi}\rangle$ prepared here appears for $\phi \neq 0$. In this case the teleportation also rotates the qubit by ϕ around the x -axis of the Bloch sphere, transforming $|\xi\rangle$ into

$$|\xi'\rangle = [\cos \frac{\phi}{2} a - i \sin \frac{\phi}{2} b] |\alpha\rangle + [\cos \frac{\phi}{2} b - i \sin \frac{\phi}{2} a] |-\alpha\rangle \quad (2)$$

Such rotations, so far considered out of experimental reach, are essential for quantum computations and Bell tests.

Implementing this protocol experimentally requires two small independent ‘‘Schrödinger kittens’’ $|c_{\pm}\rangle_{1,2}$ (Fig. 1). For $|\alpha|^2 \lesssim 1$, they can be approximated by two squeezed vacuum states $|s\rangle_{1,2}$, which can be conveniently produced by recombining the two beams emitted by an optical parametric amplifier (Fig. 2). Recombining these beams on a polarization beamsplitter (PBS1) allows us to simultaneously tap the conditioning channel for coherent photon subtraction, with a phase $\phi = \pi/2$ to produce ancillas for teleporting Hadamard gates. The two

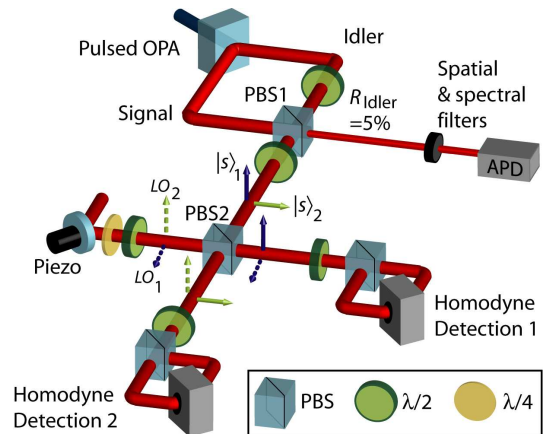


FIG. 2: Experimental setup. The signal and idler from a pulsed OPA are recombined on a polarizing beamsplitter PBS1 to produce two independent squeezed light pulses $|s\rangle_1$ and $|s\rangle_2$, while the other channel of PBS1 is used as the conditioning channel to entangle them. The two entangled beams, co-propagating with orthogonal polarizations, are separated and mixed with two local oscillators LO_1 and LO_2 on PBS2, and finally detected by two independent homodyne detections.

orthogonally polarized co-propagating modes of the prepared state are separated on PBS2 and analyzed with two independent homodyne detections.

Our OPA, described elsewhere [19], generated pairs of EPR-entangled 150-fs pulses with a 780 kHz rate, with a gain $g = \cosh^2(r_0) = 1.18$ corresponding to 3.6 dB of two-mode squeezing. The signal and idler beams were superimposed on PBS1 : $R = 5\%$ of the idler was sent into an APD counter through spatial and spectral filters, the light exiting through the other port was polarization-rotated by 45° and split on PBS2 to produce two independent squeezed vacuum pulses $|s\rangle_{1,2}$, superimposed with two local oscillators $LO_{1,2}$ (Fig. 2). The APD counts heralded single photon subtractions from the idler, performing the non-local photon annihilation $\hat{a}_1 - i\hat{a}_2$ in the two squeezed pulses and preparing the desired states with a rate $n_s \approx 600$ Hz, well above the APD dark counts ($n_d \approx 10$ Hz).

Complete two-mode tomography was performed with two homodyne detections measuring two quadratures $x_1(\theta)$ and $x_2(\phi)$, phase-controlled with waveplates and a piezo-mounted mirror. We measured 36 two-mode quadrature distributions $P_{\theta,\phi}(x_1, x_2)$, each containing $\approx 160\,000$ data points divided in 40×40 bin histograms (Fig. 3). From these distributions, using a numerical Maximal-Likelihood (MaxLike) algorithm and correcting for a finite homodyne efficiency $\eta = 70\%$, we reconstructed the density matrix $\hat{\rho}$ and the two-mode Wigner function W of the generated state. Several ‘‘cuts’’ of this function are presented on Figure 3. The value at the origin (close to 0 without correction), is clearly negative : $W(0) = -0.04 \pm 0.01$ (ideally $W(0) = \pi^{-2} \approx -0.10$).

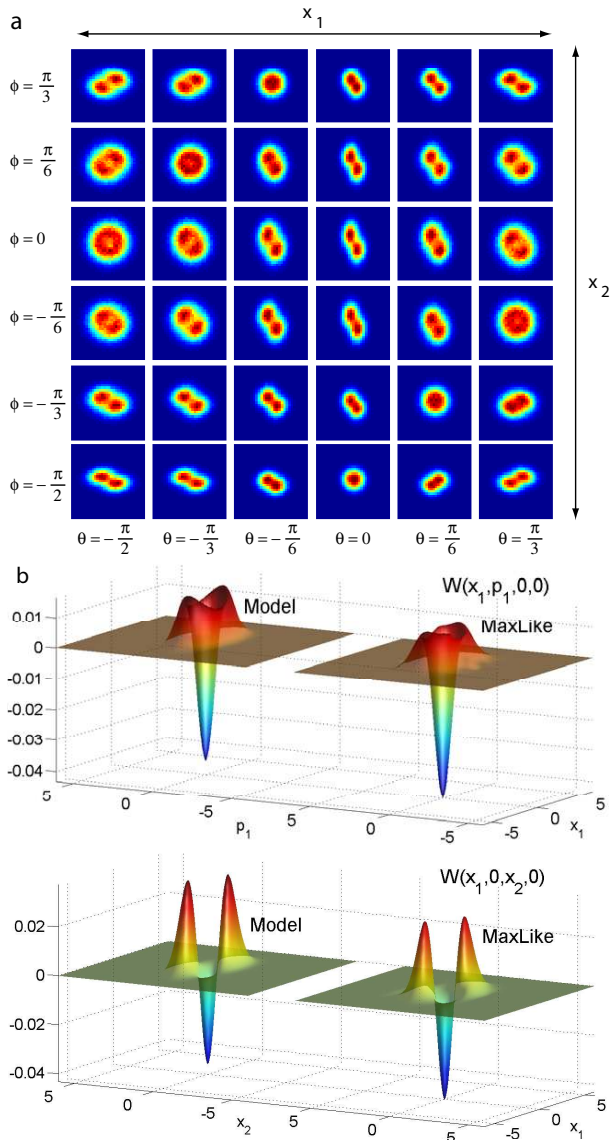


FIG. 3: (a) Experimentally measured two-mode quadrature projections. (b) Two “cuts” of the experimentally reconstructed Wigner function of the generated state (corrected for homodyne losses), compared with the prediction of our analytical model (see Supplementary Material).

This state has a fidelity $\mathcal{F} = 64 \pm 5\%$ with a pure state $|\psi_\phi\rangle$ described by $|\alpha|^2 = 0.65$ and $\phi = \pi/2$. It is mixed mostly with the non-conditioned squeezed vacuum ($\mathcal{F}_{sq} = 23 \pm 3\%$) by inconclusive APD detections. The entanglement is determined by the negativity [21] $\mathcal{N} = [||\hat{\rho}^{T_1}||_1 - 1]/2 = 0.25 \pm 0.04$ (ideally $\mathcal{N} = 0.5$). We developed a detailed analytical model (see Supplementary Materials) in excellent agreement with the experiment, both with and without correction for losses.

Remarkably, imperfections related to the photon subtraction (finite reflectivity $R = 5\%$, APD efficiency $\eta_D = 45\%$, 10 Hz dark counts) are much less detrimental than the broad OPA parametric fluorescence. The

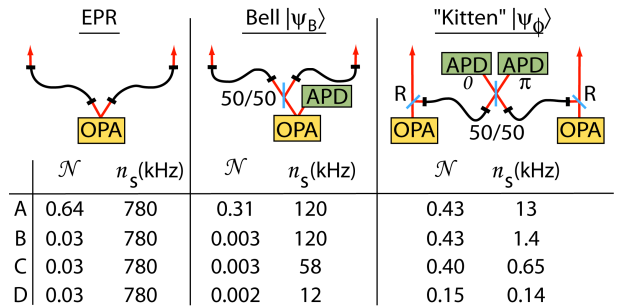


FIG. 4: Estimated entanglement \mathcal{N} and generation rate n_s of the state $|\psi_\phi\rangle$ obtained by non-local photon subtraction, compared to the direct transmission of two common entangled states generated with our setup : the initial EPR state, and the Bell state $|\psi_B\rangle$. We sequentially add various imperfections (see text for details), assuming (A) 780 kHz OPA repetition rate, 3.6 dB squeezing and $R = 5\%$, (B) 10 dB losses in each arm, (C) APDs with $n_d = 10$ Hz dark counts and $\eta_D = 45\%$ quantum efficiency, (D) broadband OPAs with $h = 1.02$, $\tau_f = 0.15$ and $\xi_f = 0.9$. We double the photon-subtraction success rate by detecting photons in the other port of the 50/50 BS and shifting by π the phase of second mode to obtain the same state $|\psi\rangle$.

excess noise it generates in the analyzed mode can be described by a phase-independent amplification of the initial squeezed vacuum, with a gain $h = 1.02$ (while $g = 1.18$) [17]. It also creates noise in other modes, resulting in unwanted APD triggers : despite tight filtering (transmission $\tau_f = 15\%$), the probability for a detected photon to come from the desired mode is $\xi_f = 0.90$. For instance, pure squeezed states would yield $\mathcal{N} = 0.48$ and a 98% fidelity with $|\psi_\phi\rangle$, despite all other imperfections. Therefore, the quality of the state is mainly limited by the specifics of our OPA, and not by the photon subtraction process.

An essential feature of this experiment is that the entanglement entirely results from the non-local photon subtraction : as expected, the tomography of the unconditioned state reveals two independent squeezed vacuum pulses with $\mathcal{N}_0 < 10^{-4} \approx 0$. The overall efficiency of the APD quantum channel used for this operation is $\tau = \eta_D \tau_f = 7\%$ dB, which corresponds to 60 km of optical fiber at telecom wavelength, i. e. to two sites separated by $2 \times 60 = 120$ km. The main contribution to these losses actually comes from the filters ($\tau_f = 15\% \equiv 40$ km), unnecessary with a narrowband OPA. But even considering them as an intrinsic defect and adding an extra 10 dB losses (2×50 km) would still yield $\mathcal{N} \approx 0.15$. By comparison, the same state prepared locally and sent through this fiber would arrive with $\mathcal{N} \approx 10^{-3}$ only.

In terms of entanglement as such, one can compare these states to others generated with the same tools. We realized a comparative experiment by sending all the idler light to the APD, conditionally preparing single photons

in the signal mode, and splitting them on a 50/50 BS between the two homodyne detections (as in Ref. [22]). The resulting state $|\psi_B\rangle = \frac{|1\rangle_1|0\rangle_2 - |0\rangle_1|1\rangle_2}{\sqrt{2}}$, ideally presenting the same entanglement, was generated 20 times faster, but even without losses its entanglement was slightly lower ($\mathcal{N} = 0.19 \pm 0.02$), due to higher photon number contributions. Sharing this state through two 50-km fibers would yield again $\mathcal{N} \approx 10^{-3}$. For the initial EPR state, \mathcal{N} would drop from 0.64 to 0.03 (Fig. 4), showing that our protocol is efficient for entanglement distribution in general.

The size of the prepared kittens, although relatively small ($|\alpha|^2 = 0.65$), is almost sufficient for the Bell test described in [13] ($|\alpha|^2 \geq 0.71$). It can be increased by using larger initial cat states $|c_{\pm}\rangle_{1,2}$, which can be generated with the same experimental tools [5, 6]. For a larger initial cats size $|\alpha|^2$, one should reduce the tapped fraction R , keeping the product $R|\alpha|^2$ constant : the fidelity and speed of the protocol are then unchanged.

This scheme overcomes, to some extent, the high sensitivity to losses encountered in many continuous-variable QIP protocols, which do not easily allow to postselect successful events. By using the specific discrete-variable advantage of discarding those events where photons were lost, we have shown that sophisticated continuous-variable entangled resources can be prepared despite strong losses in quantum channels. These states may be used as ancillas to implement arbitrary controlled qubit rotations, required in most QIP protocols, without needing strong nonlinearities or extensive experimental resources.

Acknowledgments This work is supported by the EU ICT/FET program COMPAS.

Author information The authors declare no competing financial interests. Correspondence and requests for materials should be addressed to A.O. (alexey.ourjountsev@institutoptique.fr).

[1] Schrödinger, E. Die gegenwärtige Situation in der Quantenmechanik. *Naturwissenschaften* **23**, 807 (1935).
 [2] Ourjountsev, A., Tualle-Brouri, R., Laurat, J. & Grangier, P. Generating optical Schrödinger kittens for quantum information processing. *Science* **312**, 83–86 (2006).
 [3] Neergaard-Nielsen, J. S., Nielsen, B. M., Hettich, C., Mølmer, K. & Polzik, E. S. Generation of a superposition of odd photon number states for quantum information networks. *Phys. Rev. Lett.* **97**, 083604 (2006).
 [4] Wakui, K., Takahashi, H., Furusawa, A. & Sasaki, M. Controllable generation of highly nonclassical states from nearly pure squeezed vacua. *Opt. Express* **15**, 3568–3574

(2007).
 [5] Ourjountsev, A., Jeong, H., Tualle-Brouri, R. & Grangier, P. Generation of optical “Schrödinger cats” from photon number states. *Nature* **448**, 784–786 (2007).
 [6] Takahashi, H. *et al.* Generation of large-amplitude coherent-state superposition via ancilla-assisted photon-subtraction. *arXiv:0806.2965* (2008).
 [7] Jeong, H., Kim, M. S. & Lee, J. Quantum-information processing for a coherent superposition state via a mixed entangled coherent channel. *Phys. Rev. A* **64**, 052308 (2001).
 [8] Ralph, T. C., Gilchrist, A., Milburn, G. J., Munro, W. J. & Glancy, S. Quantum computation with optical coherent states. *Phys. Rev. A* **68**, 042319 (2003).
 [9] Munro, W. J., Nemoto, K., Milburn, G. J. & Braunstein, S. L. Weak-force detection with superposed coherent states. *Phys. Rev. A* **66**, 023819 (2002).
 [10] Toscano, F., Dalvit, D. A. R., Davidovich, L. & Zurek, W. H. Sub-Planck phase-space structures and Heisenberg-limited measurements. *Phys. Rev. A* **73**, 023803 (2006).
 [11] Wenger, J., Hafezi, M., Grosshans, F., Tualle-Brouri, R. & Grangier, P. Maximal violation of bell inequalities using continuous-variable measurements. *Phys. Rev. A* **67**, 012105 (2003).
 [12] Haroche, S. *Science and ultimate reality*, chap. Breeding non-local Schrödinger cats : a thought experiment to explore the quantum-classical boundary (Cambridge University Press, Cambridge, 2004).
 [13] Stobińska, M., Jeong, H. & Ralph, T. C. Violation of Bell’s inequality using classical measurements and nonlinear local operations. *Phys. Rev. A* **75**, 052105 (2007).
 [14] Leonhardt, U. *Measuring the Quantum State of Light* (Cambridge University Press, Cambridge, 1997).
 [15] N. Lütkenhaus, Calsamiglia, J. & Suominen, K. A. Bell measurements for teleportation. *Phys. Rev. A* **59**, 3295–3300 (1999).
 [16] Duan, L.-M., Lukin, M. D., Cirac, J. I. & Zoller, P. Long-distance quantum communication with atomic ensembles and linear optics. *Nature* **414**, 413–418 (2001).
 [17] Ourjountsev, A., Dantan, A., Tualle-Brouri, R. & Grangier, P. Increasing Entanglement between Gaussian States by Coherent Photon Subtraction. *Phys. Rev. Lett.* **98**, 030502 (2007).
 [18] Enk, S. J. V. & Hirota, O. Entangled coherent states: Teleportation and decoherence. *Phys. Rev. A* **64**, 022313 (2001).
 [19] Wenger, J., Ourjountsev, A., Tualle-Brouri, R. & Grangier, P. Time-resolved homodyne characterization of individual quadrature-entangled pulses. *Eur. Phys. J. D* **32**, 391 (2005).
 [20] Wenger, J., Tualle-Brouri, R. & Grangier, P. Pulsed homodyne measurements of femtosecond squeezed pulses generated by single-pass parametric deamplification. *Opt. Lett.* **29**, 1267 (2004).
 [21] Vidal, G. & Werner, R. F. A computable measurement of entanglement. *Phys. Rev. A* **65**, 032314 (2002).
 [22] Babichev, S. A., Appel, J. & Lvovsky, A. I. Homodyne Tomography Characterization and Nonlocality of a Dual-Mode Optical Qubit. *Phys. Rev. Lett.* **92**, 193601 (2004).